



## Article

# Impact of Attitude Model, Phase Wind-Up and Phase Center Variation on Precise Orbit and Clock Offset Determination of GRACE-FO and CentiSpace-1

Junjun Yuan <sup>1,2,3</sup>, Shanshi Zhou <sup>1,3,\*</sup>, Xiaogong Hu <sup>1,3</sup>, Long Yang <sup>4</sup>, Jianfeng Cao <sup>5</sup>, Kai Li <sup>1,3</sup> and Min Liao <sup>6</sup>

<sup>1</sup> Shanghai Astronomical Observatory, Chinese Academy of Sciences, Shanghai 200030, China; yuanjunjun@shao.ac.cn (J.Y.); hxg@shao.ac.cn (X.H.); kli@shao.ac.cn (K.L.)

<sup>2</sup> University of Chinese Academy of Sciences, Beijing 100049, China

<sup>3</sup> Shanghai Key Laboratory for Space Positioning and Navigation, Shanghai 200030, China

<sup>4</sup> Beijing Future Navigation Technology Corporation Limited, Beijing 100094, China; yangl@centispace.com

<sup>5</sup> Beijing Aerospace Control and Command Center, Beijing 100089, China; jfcao@foxmail.com

<sup>6</sup> Insight Data Technology (Shenzhen) Corporation Limited, Shenzhen 518000, China; liaomin6984805@163.com

\* Correspondence: sszhou@shao.ac.cn



**Citation:** Yuan, J.; Zhou, S.; Hu, X.; Yang, L.; Cao, J.; Li, K.; Liao, M. Impact of Attitude Model, Phase Wind-Up and Phase Center Variation on Precise Orbit and Clock Offset Determination of GRACE-FO and CentiSpace-1. *Remote Sens.* **2021**, *13*, 2636. <https://doi.org/10.3390/rs13132636>

Academic Editor: Xiaoxiong Xiong

Received: 11 May 2021

Accepted: 2 July 2021

Published: 5 July 2021

**Publisher's Note:** MDPI stays neutral with regard to jurisdictional claims in published maps and institutional affiliations.

**Abstract:** Currently, low Earth orbit (LEO) satellites are attracting great attention in the navigation enhancement field because of their stronger navigation signal and faster elevation variation than medium Earth orbit (MEO) satellites. To meet the need for real-time and precise positioning, navigation and timing (PNT) services, the first and most difficult task is correcting errors in the process of precise LEO orbit and clock offset determination as much as possible. Launched in 29 September 2018, the CentiSpace-1 (CS01) satellite is the first experimental satellite of LEO-based navigation enhancement system constellations developed by Beijing Future Navigation Technology Co. Ltd. To analyze the impact of the attitude model, carrier phase wind-up (PWU) and phase center variation (PCV) on precise LEO orbit and clock offset in an LEO-based navigation system that needs extremely high precision, we not only select the CS01 satellite as a testing spacecraft, but also the Gravity Recovery and Climate Experiment Follow-On (GRACE-FO). First, the dual-frequency global positioning system (GPS) data are collected and the data quality is assessed by analyzing the performance of tracking GPS satellites, multipath errors and signal to noise ratio (SNR) variation. The analysis results show that the data quality of GRACE-FO is slightly better than CS01. With residual analysis and overlapping comparison, a further orbit quality improvement is possible when we further correct the errors of the attitude model, PWU and PCV in this paper. The final three-dimensional (3D) root mean square (RMS) of the overlapping orbit for GRACE-FO and CS01 is 2.08 cm and 1.72 cm, respectively. Meanwhile, errors of the attitude model, PWU and PCV can be absorbed partly in the clock offset and these errors can generate one nonnegligible effect, which can reach 0.02–0.05 ns. The experiment results indicate that processing the errors of the attitude model, PWU and PCV carefully can improve the consistency of precise LEO orbit and clock offset and raise the performance of an LEO-based navigation enhancement system.

**Keywords:** GRACE-FO; CentiSpace-1; attitude model; carrier phase wind-up; phase center variation



**Copyright:** © 2021 by the authors. Licensee MDPI, Basel, Switzerland. This article is an open access article distributed under the terms and conditions of the Creative Commons Attribution (CC BY) license (<https://creativecommons.org/licenses/by/4.0/>).

## 1. Introduction

In the last decade, more and more low Earth orbit (LEO) satellites operating at altitudes of 200–2000 km, such as GRACE [1], CHAMP [2], GOCE [3], SWARM [4], GRACE-FO [5], have been launched and are widely used in the geodesy and Earth fields. In addition to these traditional areas, the significance of precise orbit and clock offset determination (POCD), which are prerequisites for the success of LEO satellites' missions, has been further enlarged in the LEO navigation augmentation field [6–8]. The combination of global navigation satellite system (GNSS) and LEO data has been considered a promising

method to bring real-time and precise positioning, navigation and timing (PNT) services, such as shortening the convergence time in precise point positioning (PPP) [9–11]. In order to achieve this goal with LEO satellites, the first key point is further improving the consistency of LEO satellites' orbit and clock offset.

Because of the all-weather and high-precision characteristics of global positioning systems (GPSs), the processing of GPS observation data has become a primary method to derive the trajectories of LEO satellites, which can reach a few centimeters of uncertainty [12–15]. In the context of such high accuracy, it is a challenging task to further improve the orbit accuracy of LEO satellites. The accessibility of the attitude data of GRACE-FO provides a good opportunity to study the orbit difference between the measured and nominal attitude model [16,17]. The carrier phase wind-up (PWU) errors depend on the relative rotation between the transmitting and receiving antennas [18,19]. Mismodeled mobile receiver antenna PWU errors can reach the centimeter level [20], especially for high-speed LEO satellites. As important systematic error sources, phase center variation (PCV) errors have been deeply explored [21–23] and researchers have used direct approaches and residual approaches to obtain PCV maps [24–27]. Because of the manufacturing cost, LEO satellites often carry simple chip-scale clocks [28], which are inferior to precise GNSS atomic clocks. Any small errors may make a large difference in clock offset [6]. However, the influence of these errors on LEO satellites' clock offset is often ignored because we usually regard LEO satellites' clock offset as a parameter to be solved. Therefore, it is necessary to analyze the impact of the attitude model, PWU and PCV on LEO satellites' orbit and clock offset simultaneously, especially for LEO-based navigation systems.

Given this, the primary aim of this paper is to assess the impact of the attitude model, PWU and PCV on the orbit and clock offset determination of LEO satellites. Section 2 describes the testing spacecrafts and data quality analysis. The POCD platform and detailed strategy are discussed in Section 3. Then, we elaborate on the causes and influence of these errors in the following section. The discussion associated with the experimental results and analysis is presented in Section 4. Finally, the conclusions are presented.

## 2. Testing Spacecrafts and Data Collection

### 2.1. Testing Spacecrafts

In this study, the GRACE-FO and CentiSpace-1 satellites were selected as testing spacecrafts. The GRACE-FO [17] mission is one joint project between the National Aeronautics and Space Administration (NASA) and the German Research Centre for Geosciences (GFZ), providing continuity for the GRACE data set. Similarly to GRACE (GRACE-A and GRACE-B), the GRACE-FO consists of two satellites, GRACE-C and GRACE-D, and they are equipped with scientific instruments, such as GPS receivers and star cameras [29]. Since these two satellites are almost identical, and given the lack of data on GRACE-D in our testing period, we only select GRACE-C (abbreviated as GRCC) as one of our research objects.

The CentiSpace-1 (abbreviated as CS01) [30] is the first technology experiment satellite with an LEO satellite navigation enhancement system, developed by Beijing Future Navigation Technology Co. Ltd. The CS01 satellite is equipped with a GNSS receiver and laser inter-satellite crosslink instrument. The primary mission of CS01 is to explore the capability of the LEO-based augmentation system. This enhancement system will consist of more than 120 LEO satellites and deliver high accuracy and low-cost service [31].

### 2.2. Data Collection and Quality Analysis

The high-quality GPS data are of great significance to LEO satellites, so we analyzed the data quality before POCD. Onboard GPS data with a 10 s sampling rate from day of year (DOY) 273 to 278, 2018, were collected. First, the number of observed and useful satellites was discussed. In this paper, the number of observed satellites means the sum of all satellites tracked by the LEO receiver at one epoch and the useful number is defined as the sum of all satellites for which both code and phase dual-frequency data are simultaneously

available. From the top panel of Figure 1, we can see that the average observed satellite number of CS01 is much higher than that of GRCC. The largest observed number of GRCC and CS01 is 10 and 12, respectively. The proportion of tracking 6 to 10 GPS satellites for GRCC is 99.81% and the proportion of tracking 10 to 12 GPS satellites for CS01 is as high as 99.38%. In the performance of useful satellites, GRCC is better than CS01, as seen in the bottom panel of Figure 1. The percentage of 4–6 useful satellites for GRCC and CS01 in an epoch is 2.10% and 4.40%, respectively. However, the percentage of 7–12 useful satellites for GRCC and CS01 in an epoch is 97.89% and 95.39%, respectively.

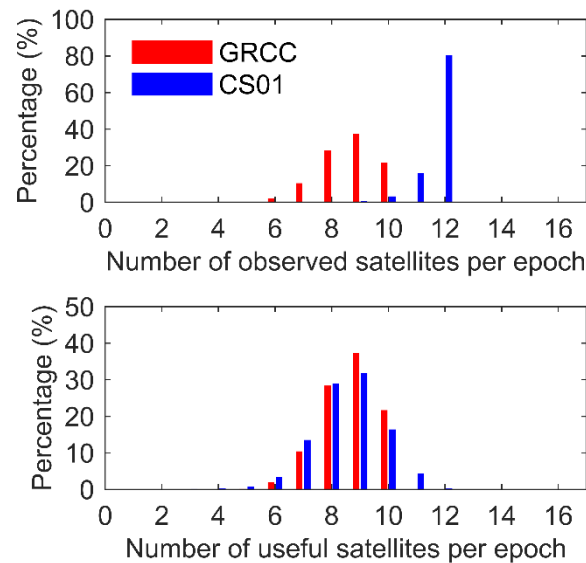


**Figure 1.** Average percentage of observed (**top**) and useful (**bottom**) GPS satellites for GRCC and CS01.

As an important index of assessing systematic errors in an LEO receiver [16,22], multipath errors for GRCC and CS01 are analyzed. The code multipath errors of P1 and P2, recorded as MP1 and MP2, are determined by TEQC [32]. Figure 2 shows the variation in the code multipath error with the elevation angle for GRCC and CS01 in DOY 273, 2018. Whether GRCC or CS01 satellite, both MP1 and MP2 tend to be smaller, with a larger elevation angle, indicating one elevation-dependent pattern, and the average MP1 series was found to be smaller than MP2. However, the multipath errors of GRCC can decrease faster than CS01 with increasing elevation angle ( $\geq 20^\circ$ ). Another noticeable phenomenon is that the average multipath errors for CS01 are larger than GRCC, where the root mean square (RMS) of L1 and L2 multipath error for GRCC is 0.12 m, 0.17 m, respectively, and the corresponding values for CS01 are 0.26 m, 0.38 m, respectively. In addition, we note that it is difficult for CS01 to track GPS satellites at low elevations ( $\leq 5^\circ$ ). The reason may be related to the manufacturing characteristics of the receiver itself.

Figure 3 displays the average signal to noise ratio (SNR) series with elevations for GRCC and CS01. As for GRCC, the general variations between SNR and elevations are quite stable. However, the SNR of CS01 tends to be larger with increasing elevation. Overall, the data quality of GRCC is somewhat superior to that of CS01. However, taking manufacturing costs into consideration, the performance of CS01 is still satisfactory compared to GRCC.

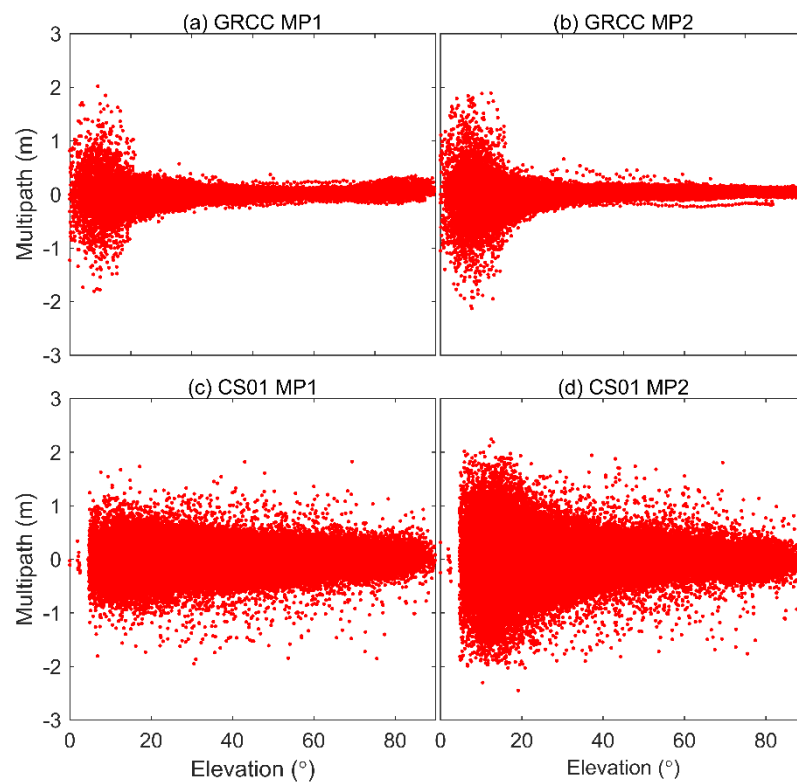


Figure 2. Multipath error variations with elevation for GRCC and CS01.

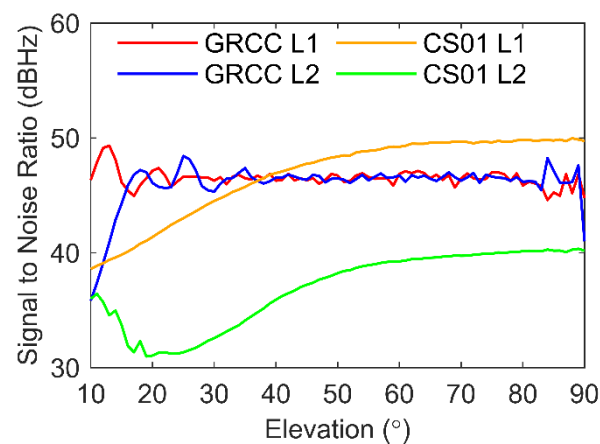


Figure 3. Signal to noise ratio series with elevation for GRCC and CS01.

### 3. POCD Platform and Strategy

Since the 1990s, the Shanghai Astronomical Observatory of Chinese Academy of Sciences has carried out a series of studies on GNSS and LEO data processing, and abundant experience and knowledge has been accumulated. The Shanghai Astronomical Observatory Orbit Determination (SHAOOD) software is written in FORTRAN language with a unified code style. To improve the overall solution efficiency, the clock offset reduction algorithm [33] is added to the least square batch processing. Users only need to change the parameters of the configuration card and provide the necessary files to realize the personalized solution.

With SHAOOD software, we model the perturbation forces to achieve the best results. The ionosphere-free pseudo range combination (PC) and carrier phase combination (LC) are formed to eliminate first-order ionospheric delay error. For GPS precise orbit and clock offset, the final orbit and clock offset products from the Center for Orbit Determination in

Europe (CODE) [34] are used. Additionally, we use the International GNSS Service (IGS) model from “igs14.atx” [35] to correct the GPS Phase Center Offset (PCO) and PCV. As for GPS observations, the cut-off elevation angle is set to  $5^\circ$  and the data sampling rate is 10 s. The LEO attitude model, PWU and PCV corrections will be discussed and analyzed in the following section. Table 1 provides more detailed information about the measurement models, dynamic models and estimated parameters.

**Table 1.** Processing strategies for testing spacecrafts.

Model	Description
<b>Measurement model</b>	
Observation	Non-differentiated ionosphere-free linear combination
Arc length and interval	12 h, 10 s
Weighting strategy	PC (a priori sigma of 1 m), LC (a priori sigma of 1 cm)
GPS products	CODE final products [34]
Elevation cut-off angle	$5^\circ$
GNSS PCO and PCV	igs14.atx [35]
LEO attitude	Discussed
Phase wind-up	Discussed
LEO PCO and PCV	Nominal values; Discussed
<b>Dynamic model</b>	
Earth gravity	EIGEN_GL04C, $120 \times 120$ [36]
N-body	JPL DE405 [37]
Relativity	IERS 2010 [38]
Solid earth tide and pole tide	IERS 2010 [38]
Ocean tides	FES 2004, $30 \times 30$ [39]
Solar radiation pressure	Cannonball model [40]
Atmospheric drag	NRLMSISE-00 [41], piecewise periodical estimation
Empirical forces	Piecewise periodical estimation of the sin and cos coefficients in the track and normal directions
<b>Estimated parameters</b>	
LEO initial state	Position and velocity at the initial state
Receiver clock	Epoch-wise estimated
Ambiguities	Floated solution
Solar coefficients	One per 3 h
Drag coefficients	One per 3 h
Empirical coefficients	One per 3 h

#### 4. Results and Discussion

During the testing period (DOY 273–278, 2018), the orbits of GRCC and CS01 were generated every 2 h and there were 67 sets of results. Because there were no external measurements for CS01, post-fit phase residuals and orbit overlap differences were used to evaluate the CS01 orbit’s consistency. In addition to the above evaluation methods, Jet Propulsion Laboratory (JPL) orbit comparison was adopted for GRCC. The overlap time between two adjacent arcs was 10 h, and to avoid the effect of edge, the central 8 h arcs were used for analysis.

#### 4.1. Impact of Attitude Model

##### 4.1.1. Attitude Modeling

First, we give the definition of the satellite body-fixed (SBF) of GRCC and CS01. The origin of GRCC's SBF is the center of mass of the Super STAR Accelerometer proof mass, which almost coincides with GRCC's center of mass. The +X axis (roll axis) is defined from the origin to the phase center of the K/Ka band horn; the +Y axis (pitch axis) comprises a right-handed triad with the +X and +Z axis; +Z (Yaw Axis) is normal to the plane of the main equipment platform and positive towards the satellite radiator [17]. For CS01, the origin of SBF is the center of mass. The +X axis is aligned to the satellite positive velocity direction; the +Z axis points toward the Earth's center of mass, and the +Y axis is perpendicular to the XOZ plane, completing the right-hand coordinate system. GPS observations involve the geometric range between the antenna phase center location of the GPS satellite (transmitting end) at signal emission time and the antenna phase center location of the LEO satellite (receiving end) at signal reception time, whereas the final POCD results are based on the center of mass (COM). Meanwhile, the PCO values usually are defined in SBF, but the orbits should be computed in a conventional terrestrial system (CTS). Therefore, the attitude transformation matrix  $R$  between SBF and CTS is of great importance to the accuracy of LEO satellites' orbit. The GRACE-FO satellites provide measured attitude model data in the form of rotation quaternions that are composed of four elements,  $q_1, q_2, q_3$  and  $q_4$ . The first three are vector parts, providing the orientation along the roll, pitch and yaw axis, respectively, and the last one is the scalar part. Therefore, we can obtain the transformation matrix  $R$  based on the quaternions, which can be expressed as follows:

$$R = \begin{pmatrix} q_4^2 + q_1^2 - q_2^2 - q_3^2 & 2(q_1q_2 - q_3q_4) & 2(q_1q_3 - q_2q_4) \\ 2(q_1q_2 + q_3q_4) & q_4^2 - q_1^2 + q_2^2 - q_3^2 & 2(q_2q_3 - q_1q_4) \\ 2(q_1q_3 - q_2q_4) & 2(q_2q_3 - q_1q_4) & q_4^2 - q_1^2 - q_2^2 + q_3^2 \end{pmatrix}$$

Note that, in the testing period in this paper, GRCC is in the leading position and the +X axis of the GRCC satellite is in the anti-flight direction. For CS01, the measured attitude data are not available. However, in SHAOOD software, transformations between CTS and SBF can be performed using measured or nominal attitude [42] according to the actual needs. Therefore, this part of the research on the attitude model will mainly focus on GRCC.

##### 4.1.2. Validation and Discussion

Due to the stable attitude control for GRACE-FO, the difference in the phase center vectors between two solutions is small (seen Figure 4). The average RMS of phase center vectors in the x, y, z direction is 4.72 mm, 3.88 mm and 5.08 mm, respectively. To analyze the influence of the attitude model, two sets of orbit and clock offset using nominal and measured attitude data for GRCC are generated. The impact of different attitude models on POCD is given in Figure 5, and Table 2 summarizes the RMS of the orbit differences and residual. The average RMS of radial (R), along-track (T), cross-track (N) and three-dimensional (3D) position accuracy of overlap comparison using the nominal attitude model are 0.75 cm, 1.56 cm, 1.26 cm and 2.15 cm, respectively. Additionally, the average RMS of the R, T, N and 3D positions' accuracy using the measured attitude model are 0.75 cm, 1.55 cm, 1.24 cm and 2.14 cm, respectively. A slight improvement can be also observed in the JPL orbit comparison. As for phase residuals, the average RMS using the measured attitude improves from 7.95 to 7.93 mm.

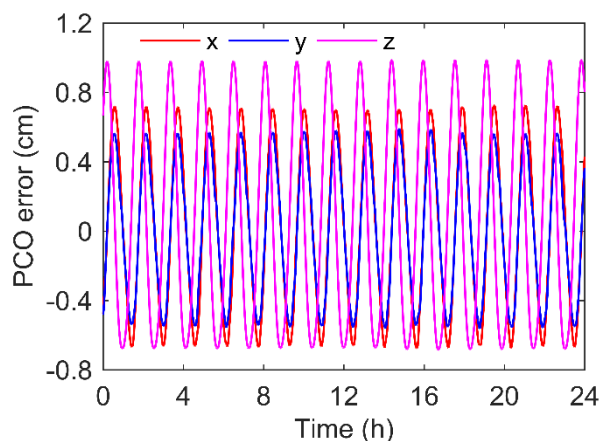


**Figure 4.** The difference in phase center vectors in CTS frame using nominal and measured attitude. DOY 273, 2018.

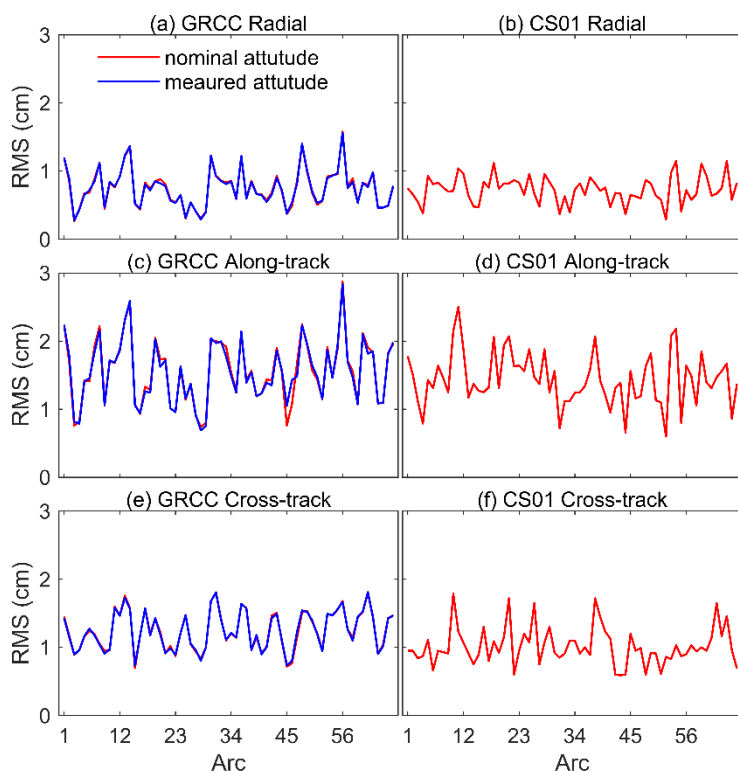


**Figure 5.** RMS of orbital differences for GRCC and CS01 using nominal and measured attitude model.

**Table 2.** The RMS of residual and orbital comparison using nominal and measured attitude for GRCC and CS01.

Spacecraft	Solutions	Residual (mm)	Overlap Comparison (cm)				JPL Comparison (cm)			
			R	T	N	3D	R	T	N	3D
GRCC	Nominal ATT	7.95	0.75	1.56	1.25	2.15	2.07	2.08	1.15	3.18
	Measured ATT	7.93	0.75	1.55	1.24	2.14	2.06	2.07	1.15	3.17
CS01	Nominal ATT	9.37	0.72	1.44	1.01	1.93	/	/	/	/
	Measured ATT	/	/	/	/	/	/	/	/	/

The difference in clock offset using nominal and measured attitude is shown in Figure 6. The average RMS can reach 0.023 ns, which is an important difference for users who wish to use the products of the LEO-based enhancement system. We introduce a signal-in-space

range error (SISRE) to quantify this impact. Orbital errors  $\Delta r = (\Delta r_R, \Delta r_T, \Delta r_N)$ , which are described in the  $R, T$  and  $N$  directions, can be expressed as a weighted average of RMS errors. These orbital errors vary with the orientation of the line-of-sight vector  $e$  and the user location. The combined orbit and clock SISRE can be expressed by [7,43]

$$\text{SISRE} = \sqrt{[\text{RMS}(w_R \Delta r_R - \Delta cdt)]^2 + w_{A,C}^2 \left( (\text{RMS} \Delta r_T)^2 + (\text{RMS} \Delta r_N)^2 \right)}$$

where  $\Delta cdt$  is the error in the clock offset; the weight factors  $w_R^2$  and  $w_{A,C}^2$  are altitude-dependent and we compute the weight factors using the scheme from [43]. For the GRCC satellite,  $w_R^2 = 0.4557$  and  $w_{A,C}^2 = 0.6294$ . For the CS01 satellite,  $w_R^2 = 0.5153$  and  $w_{A,C}^2 = 0.6060$ . The combined orbit and clock SISRE for GRCC caused by the attitude model is 0.69 cm. On one hand, the attitude control of GRACE and GRACE-FO is very stable [13,44], and the measured attitude model is close to the nominal attitude model. On the other hand, the results also indicate that the potential to implement measured and nominal attitude in SHAOOD software is high. However, the errors of the attitude model can be partly absorbed in the orbit and clock error. Therefore, it is still necessary to use the precise measured attitude model, if available.

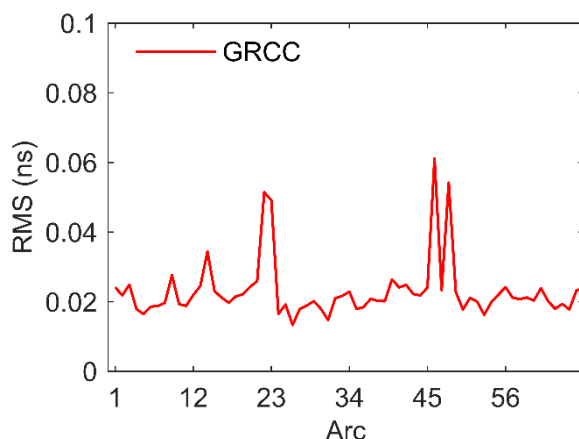


Figure 6. The difference in GRCC’s clock offset between solutions using nominal and measured attitude.

#### 4.2. Impact of Phase Wind-Up

##### 4.2.1. Carrier Phase Wind-Up Effect

The electromagnetic wave emitted by GPS satellites is typically in the form of right-hand circular polarization (RHCP). Relative rotation of the transmitting or receiving antennas will change the carrier phase, which is called the phase wind-up (PWU) effect. Note that this error only affects the phase observations and not the pseudo range. We compute the PWU corrections ( $\omega$ ) using the following expressions [18]:

$$\begin{aligned} D &= x - k(k \cdot x) + k \times y \\ \bar{D} &= \bar{x} - k(k \cdot \bar{x}) - k \times \bar{y} \\ \omega &= \text{sign}(k \cdot (\bar{D} \times D)) \arccos \left( \frac{\bar{D} \cdot D}{|\bar{D}| |D|} \right) \end{aligned}$$

where  $D, \bar{D}$  are the effective dipole vectors of the transmitter and receiver antenna, respectively;  $k$  is the unit vector pointing from transmitter to receiver antenna;  $x, y$  are the corresponding dipole unit vectors of the transmitting antenna and  $\bar{x}, \bar{y}$  are the corresponding dipole unit vectors of the receiving antenna.

First, PWU corrections can be absorbed by epoch-wise estimation parameters if uncorrected, and they are finally reflected in the accuracy of orbit and clock offset. Second,

the PWU effects can be divided into two categories: the PWU caused by the rotation of the transmitting antenna and the PWU caused by the rotation of the receiving antenna [20]. The ground receiver antenna always remains in a static state and remains oriented towards a fixed reference direction (usually north). The local east north up (ENU) coordinates can be used for the ground receiver, and the corresponding dipole unit vectors of the receiving antenna can be defined as pointing to the east and north [19]. This means that only the PWU caused by the rotation of the transmitting antenna is taken into consideration. However, the LEO antenna in high-speed motion also has relative rotation. Thus, the receiver orientation must be carefully defined to calculate the correct PWU. In this paper, we use SBF coordinates to define the corresponding dipole unit vectors of the receiving antenna instead of ENU coordinates.

#### 4.2.2. Validation and Discussion

Figure 7 shows the PWU variations for GRCC and CS01 in DOY 273, 2018. It can be clearly seen that the average PWU error for GRCC is smaller than CS01 and the overall fluctuation trend of GRCC is more stable. For GRCC, the average RMS of PWU is 3.84 cm, while the value is 4.77 cm for CS01. This means that the performance of attitude control in GRCC is superior to that of CS01.

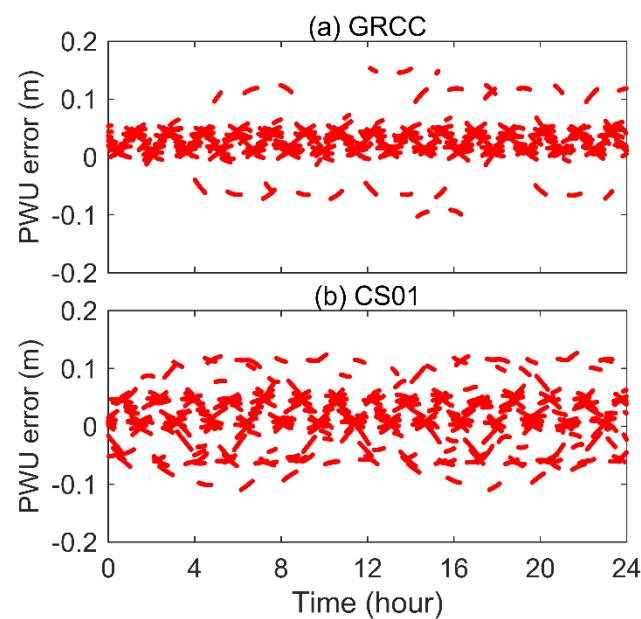


Figure 7. The PWU variations for GRCC and CS01 in DOY 273, 2018.

Figure 8 shows the overlap difference in RMS between solutions with and without PWU corrections for GRCC and CS01, and Table 3 lists the corresponding statistical results. Without PWU correction, the 3D RMS of overlap for GRCC and CS01 is 2.15 cm, 1.93 cm, respectively. Adding the PWU correction leads to improvements, with 3D RMS values for GRCC and CS01 of 2.11 cm, 1.88 cm, respectively. The RMS of the phase residual for GRCC and CS01 can be improved by 0.12 mm and 0.06 mm, respectively. The improvement reflected in the orbit comparison with JPL orbit differences for GRCC is more obvious, with 3D RMS values decreasing from 3.17 cm to 2.98 cm. Meanwhile, the clock offset difference in RMS (seen in Figure 9) for GRCC and CS01 is 0.047 ns, 0.052 ns, respectively. The combined orbit and clock SISRE for GRCC and CS01 caused by PWU corrections can reach up to 1.42 cm and 1.57 cm, respectively. This means that more PWU errors have a significant impact on the service capability of an LEO-based navigation enhancement system. Therefore, the PWU corrections must be taken into consideration in the precise orbit and clock offset determination.

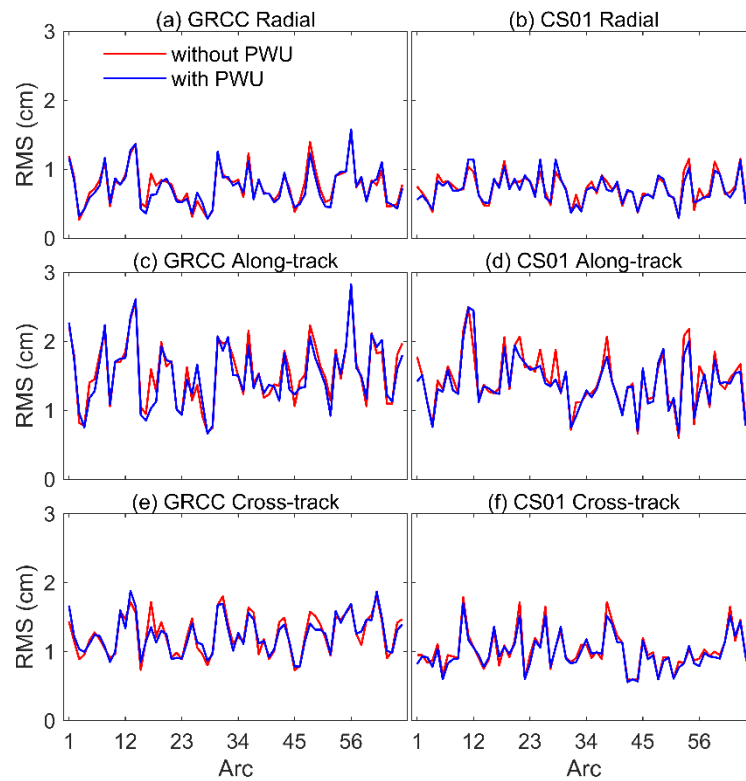


Figure 8. RMS of orbital differences for GRCC and CS01 with/without PWU corrections.

Table 3. The RMS of residual and orbital comparison with/without PWU for GRCC and CS01.

Spacecraft	Solutions	Residual (mm)	Overlap Comparison (cm)				JPL Comparison (cm)			
			R	T	N	3D	R	T	N	3D
GRCC	without PWU	7.93	0.75	1.56	1.25	2.15	2.07	2.08	1.15	3.17
	with PWU	7.81	0.73	1.52	1.24	2.11	1.89	1.91	1.23	2.98
CS01	without PWU	9.37	0.72	1.44	1.01	1.93	/	/	/	/
	with PWU	9.31	0.71	1.39	0.98	1.88	/	/	/	/

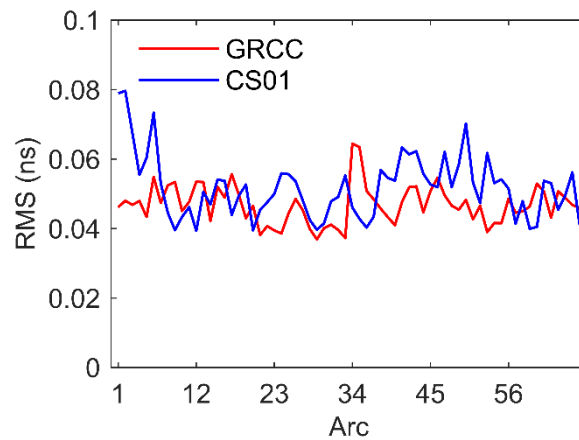


Figure 9. The difference in clock offset between solutions with and without PWU corrections.

### 4.3. Impact of PCV

#### 4.3.1. Estimation of PCV Maps

Precise phase center modeling of the LEO receiver antenna is of importance in the performance of LEO satellite missions. Taking the electrical phase center as a single

point is no longer possible in high-precision applications when the signal wave front fluctuates because of the antenna manufacturing characteristics. Although PCV values may be provided in advance, there will be a difference between the in-flight and ground calibration values because of the special space environment, satellite mass change and other reasons [23]. First, to avoid the influence of GPS satellites' PCO and PCV, we introduce precise values from the antenna information exchange file (igs14.atx) provided by IGS [35]. After the PCO of LEO antennas is fixed, we use post-fit phase residuals of GPS ionosphere-free phase measurements (DOY 273-293, 2018) by iterations until convergence, namely the residual approach [24,25], to estimate the PCV maps and analyze its impact.

The PCV maps ( $5^\circ \times 5^\circ$ ) of GRCC and CS01 in the Antenna Reference Frame (ARF) system obtained by the residual approach are displayed in Figure 10. The azimuth of  $0^\circ$  (X-axis) nominally points in the flight direction, but it should be noted that the X-axis of GRCC is opposite in our testing period. For GRCC, the overall scale is limited to  $-6$  mm to  $+10$  mm, with extreme values of  $-5.56$  mm and  $+8.81$  mm, respectively. The PCV maps of CS01 use the same scale of  $-10$  to  $10$  mm, but with extreme values of  $-10.27$  mm and  $26.32$  mm. The overall deeper colors of the CS01 PCV maps compared to the GRCC mean that the PCV values of CS01 are larger than GRCC. In addition, the PCV map of CS01 has a stronger elevation-dependent pattern than GRCC.

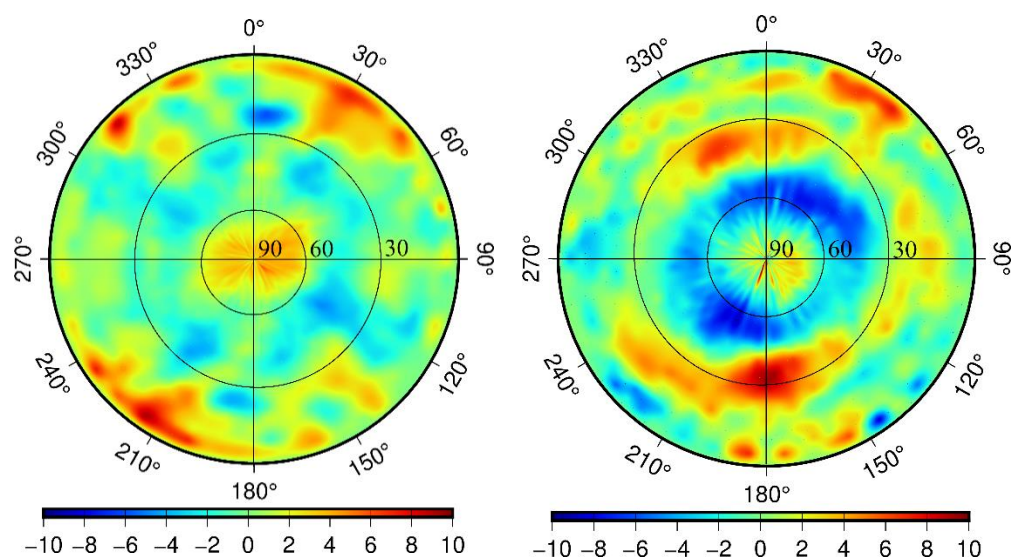


**Figure 10.** Azimuth-elevation maps of the  $5^\circ \times 5^\circ$  PCV (mm) for the ionosphere-free linear combination of the GRCC (left) and CS01 (right).

#### 4.3.2. Validation and Discussion

Comparing solutions without and with PCV corrections, the improvement of overlap orbit comparisons by PCV estimation is analyzed (see Figure 11) and the RMS values of residual analysis and orbit comparisons in the R, T, N and 3D directions are listed in Table 4. For GRCC, the mean RMS of the dynamic post-fit residual can be significantly reduced from 7.81 mm to 7.31 mm by applying the PCV model. When considering PCV corrections, the accuracy improvements in the 3D RMS of overlap orbit comparison and JPL orbit comparison amount to 0.3 mm and 2.3 mm, respectively. For CS01, with larger PCV scales, the post-fit residual can be reduced from 9.31 mm to 8.55 mm, and the accuracy of the 3D RMS of overlap orbit comparison can be improved from 1.88 cm to 1.72 cm. Meanwhile, the PCV corrections also can significantly affect the consistency of clock offset (see Figure 12), where the RMS of the clock offset difference for GRCC and CS01 is 0.043 ns and 0.027 ns, respectively. The combined orbit and clock SISRE for GRCC and CS01 caused by PCV corrections is 1.30 cm and 0.86 cm, respectively. This shows that applying phase residual estimations for ionosphere-free PCV correction is necessary in high-precision LEO orbit and clock offset determination.

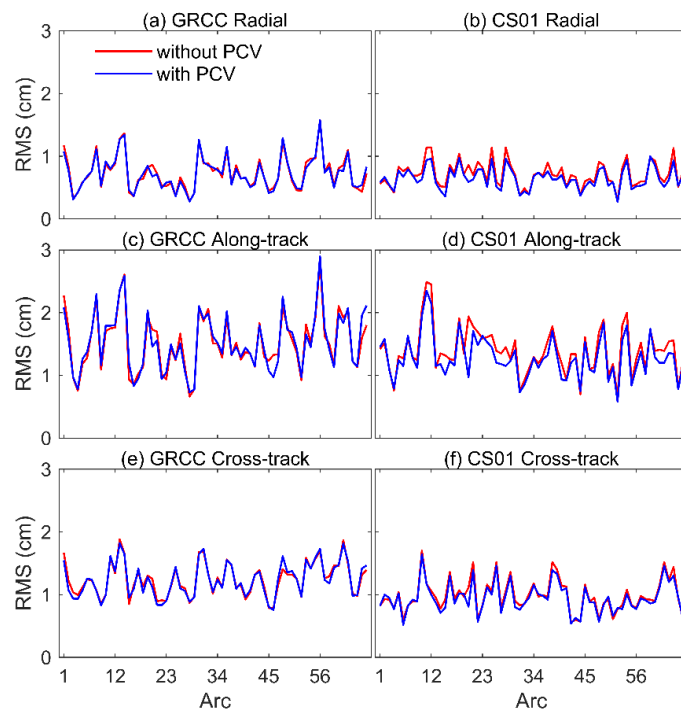


Figure 11. RMS of orbital differences for GRCC and CS01 with/without PCV corrections.

Table 4. The RMS of residual and orbital comparison with/without PCV for GRCC and CS01.

Spacecraft	Solutions	Residual (mm)	Overlap Comparison (cm)				JPL Comparison (cm)			
			R	T	N	3D	R	T	N	3D
GRCC	without PCV	7.81	0.73	1.52	1.24	2.11	1.89	1.91	1.23	2.98
	with PCV	7.31	0.72	1.50	1.23	2.08	1.78	1.63	1.29	2.75
CS01	without PCV	9.31	0.71	1.39	0.98	1.88	/	/	/	/
	with PCV	8.55	0.65	1.28	0.95	1.72	/	/	/	/

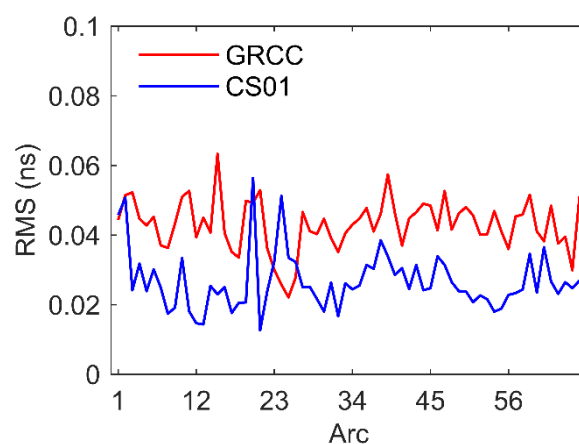


Figure 12. The difference in clock offset between solutions with and without PCV corrections.

### 5. Conclusions

This paper systematically discusses the impact of an attitude model, PWU and PCV on the precise orbit and clock offset of GRCC and CS01 satellites, as well as the GPS data quality. First, we studied the space-borne GPS data quality of GRCC and CS01 from the performance of tracking GPS satellites, multipath errors and SNR variation. The overall data quality of GRCC is superior to that of CS01 because of manufacturing characteristics

and cost. The precise orbit and clock offset play a very important role in the LEO-based navigation enhancement system and the errors of the attitude model, PWU and PCV cannot be neglected. After correcting the errors of the attitude model, PWU and PCV, the orbit quality was further improved, as evidenced by residual analysis and overlap comparison. The final GRCC and CS01 orbit consistency (3D RMS) can reach up to 2.08 cm and 1.72 cm, respectively, which satisfies the high-precision requirement of LEO-based navigation enhancement systems. The impact of the attitude model, PWU and PCV on the clock offset of GRCC is 0.023 ns, 0.047 ns and 0.043 ns, and the impact of PWU and PCV on the clock offset of CS01 is 0.052 ns and 0.027 ns, respectively. For LEO-based navigation enhancement systems, the orbit and clock offset determine the overall performance. Small errors in the attitude model, PWU and PCV can also have nonnegligible effects on LEO orbit and clock offset. Therefore, the clock offset of LEO satellites should be given great attention in LEO-based navigation systems, not considered simple estimated parameters. Furthermore, this paper also shows that there is still room for improvement for LEO orbit and clock offset if we can process the attitude model, PWU and PCV carefully. Meanwhile, the orbit determination capability of our SHAOOD software was explored, and it can achieve centimeter level orbit determination accuracy. The research results of this paper can provide a reference for the construction of an LEO-based satellite navigation system.

**Author Contributions:** J.Y. wrote the article and processed the data, S.Z. designed the experiments, L.Y. provided original data and suggestions, X.H., J.C., K.L. and M.L. contributed to discussions and revisions. All authors have read and agreed to the published version of the manuscript.

**Funding:** This research received no external funding.

**Data Availability Statement:** All GRACE-FO data in this paper can be freely accessed at <ftp://isdctf.gfz-potsdam.de/grace-fo/> (accessed on 11 March 2021). The GPS ephemeris and clock products can be found at <ftp://ftp.aiub.unibe.ch/CODE/> (accessed on 11 March 2021). The GPS antenna file can be found at <ftp://igs.ign.fr/pub/igs/igs/scb/station/general/> (accessed on 11 March 2021).

**Acknowledgments:** Beijing Future Navigation Technology Co. Ltd. is gratefully acknowledged for providing CentiSpace-1 GPS data. The authors thank GFZ for providing GRACE-FO GPS data. And the authors are grateful to the CODE and IGS for providing GPS products and other necessary products. The authors thank the reviewers and editors for constructive comments and works that have improved the quality of this manuscript.

**Conflicts of Interest:** The authors declare no conflict of interest.

## References

1. Tapley, B.D.; Bettadpur, S.; Watkins, M.; Reigber, C. The gravity recovery and climate experiment: Mission overview and early results. *Geophys. Res. Lett.* **2004**, *31*. [[CrossRef](#)]
2. Reigber, C.; Lühr, H.; Schwintzer, P. CHAMP mission status. *Adv. Space Res.* **2002**, *30*, 129–134. [[CrossRef](#)]
3. Bock, H.; Jäggi, A.; Meyer, U.; Visser, P.; Ijssel, J.V.D.; Van Helleputte, T.; Heinze, M.; Hugentobler, U. GPS-derived orbits for the GOCE satellite. *J. Geod.* **2011**, *85*, 807–818. [[CrossRef](#)]
4. Ijssel, J.V.D.; Encarnação, J.; Doornbos, E.; Visser, P. Precise science orbits for the Swarm satellite constellation. *Adv. Space Res.* **2015**, *56*, 1042–1055. [[CrossRef](#)]
5. Kornfeld, R.P.; Arnold, B.W.; Gross, M.A.; Dahya, N.T.; Klipstein, W.M.; Gath, P.F.; Bettadpur, S. Grace-fo: The gravity recovery and climate experiment follow-on mission. *J. Spacecr. Rocket.* **2019**, *56*, 931–951. [[CrossRef](#)]
6. Yang, Z.; Liu, H.; Qian, C.; Shu, B.; Zhang, L.; Xu, X.; Zhang, Y.; Lou, Y. Real-time estimation of low earth orbit (LEO) satellite clock based on ground tracking stations. *Remote Sens.* **2020**, *12*, 2050. [[CrossRef](#)]
7. Reid, T.G.; Neish, A.M.; Walter, T.F.; Enge, P.K. Leveraging commercial broadband LEO constellations for navigating. In Proceedings of the ION GNSS+ 2016, Portland, OR, USA, 12–16 September 2016; pp. 2300–2314.
8. Li, B.; Ge, H.; Ge, M.; Nie, L.; Shen, Y.; Schuh, H. LEO enhanced global navigation satellite system (LeGNSS) for real-time precise positioning services. *Adv. Space Res.* **2019**, *63*, 73–93. [[CrossRef](#)]
9. Li, X.; Ma, F.; Li, X.; Lv, H.; Bian, L.; Jiang, Z.; Zhang, X. LEO constellation-augmented multi-GNSS for rapid PPP convergence. *J. Geod.* **2019**, *93*, 749–764. [[CrossRef](#)]
10. Zhang, X.; Ma, F. Review of the development of LEO navigation-augmented GNSS. *Acta Geod. Cartogr. Sin.* **2019**, *48*, 1073–1087. [[CrossRef](#)]

11. Guan, M.; Xu, T.; Gao, F.; Nie, W.; Yang, H. Optimal walker constellation design of LEO-based global navigation and augmentation system. *Remote Sens.* **2020**, *12*, 1845. [CrossRef]
12. Kang, Z.; Tapley, B.; Bettadpur, S.; Ries, J.; Nagel, P. Precise orbit determination for GRACE using accelerometer data. *Adv. Space Res.* **2006**, *38*, 2131–2136. [CrossRef]
13. Kang, Z.; Nagel, P.; Pastor, R. Precise orbit determination for GRACE. *Adv. Space Res.* **2003**, *31*, 1875–1881. [CrossRef]
14. Jäggi, A.; Hugentobler, U.; Bock, H.; Beutler, G. Precise orbit determination for GRACE using undifferenced or doubly differenced GPS data. *Adv. Space Res.* **2007**, *39*, 1612–1619. [CrossRef]
15. Montenbruck, O.; Hackel, S.; Jäggi, A. Precise orbit determination of the Sentinel-3A altimetry satellite using ambiguity-fixed GPS carrier phase observations. *J. Geod.* **2018**, *92*, 711–726. [CrossRef]
16. Hwang, C.; Tseng, T.-P.; Lin, T.-J.; Švehla, D.; Hugentobler, U.; Chao, B.F. Quality assessment of Formosat-3/Cosmic and grace GPS observables: Analysis of multipath, ionospheric delay and phase residual in orbit determination. *GPS Solut.* **2009**, *14*, 121–131. [CrossRef]
17. Wen, H.; Kruizinga, G.; Paik, M.; Landerer, F.; Bertiger, W.; Sakumura, C.; Bandikova, T.; McCullough, C. *Technical Report JPL D-56935: Grace-Fo Level-1 Data Product User Handbook*; Jet Propulsion Laboratory: Pasadena, CA, USA, 2019.
18. Wu, J.T.; Wu, S.C.; Hajj, G.A.; Bertiger, W.I.; Lichten, S.M. Effects of antenna orientation on GPS carrier phase. *Astrodynamic* **1992**, *1992*, 1647–1660.
19. Kouba, J. A Guide to Using International GNSS Service (IGS) Products. Available online: <https://igsceb.jpl.nasa.gov/igsceb/resource/pubs/Using/IGSPProductsVer21.pdf> (accessed on 10 December 2017).
20. Cai, M.; Chen, W.; Dong, D.; Yu, C.; Zheng, Z.; Zhou, F.; Wang, M.; Yue, W. Ground-based phase wind-up and its application in yaw angle determination. *J. Geod.* **2016**, *90*, 757–772. [CrossRef]
21. Montenbruck, O.; Garcia-Fernandez, M.; Yoon, Y.; Schön, S.; Jäggi, A. Antenna phase center calibration for precise positioning of LEO satellites. *GPS Solut.* **2008**, *13*, 23–34. [CrossRef]
22. Guo, J.; Zhao, Q.; Guo, X.; Liu, X.; Liu, J.; Zhou, Q. Quality assessment of onboard GPS receiver and its combination with DORIS and SLR for Haiyang 2A precise orbit determination. *Sci. China Earth Sci.* **2015**, *58*, 138–150. [CrossRef]
23. Gu, D.; Lai, Y.; Liu, J.; Ju, B.; Tu, J. Spaceborne GPS receiver antenna phase center offset and variation estimation for the Shiyang 3 satellite. *Chin. J. Aeronaut.* **2016**, *29*, 1335–1344. [CrossRef]
24. Jäggi, A.; Dach, R.; Montenbruck, O.; Hugentobler, U.; Bock, H.; Beutler, G. Phase center modeling for LEO GPS receiver antennas and its impact on precise orbit determination. *J. Geod.* **2009**, *83*, 1145–1162. [CrossRef]
25. Bock, H.; Jäggi, A.; Meyer, U.; Dach, R.; Beutler, G. Impact of GPS antenna phase center variations on precise orbits of the GOCE satellite. *Adv. Space Res.* **2011**, *47*, 1885–1893. [CrossRef]
26. Mao, X.; Visser, P.; Ijssel, J.V.D. Impact of GPS antenna phase center and code residual variation maps on orbit and baseline determination of GRACE. *Adv. Space Res.* **2017**, *59*, 2987–3002. [CrossRef]
27. Yuan, J.; Zhao, C.; Wu, Q. Phase center offset and phase center variation estimation in-flight for ZY-3 01 and ZY-3 02 space-borne GPS antennas and the influence on precision orbit determination. *Acta Geod. Cartogr. Sin.* **2018**, *47*, 672–682. [CrossRef]
28. Hein, G.W. Status, perspectives and trends of satellite navigation. *Satell. Navig.* **2020**, *1*, 1–12. [CrossRef]
29. Landerer, F.; Flechtner, F.; Webb, F.; Watkins, M.; Save, H.; Bettadpur, S.; Gaston, R. *Grace Following-On: Mission Status and First Mass Change Observations*; IUGG: Montreal, QC, Canada, 2019.
30. Su, M.; Su, X.; Zhao, Q.; Liu, J. BeiDou augmented navigation from low earth orbit satellites. *Sensors* **2019**, *19*, 198. [CrossRef]
31. Yang, L. The centospace-1: A leo satellite-based augmentation system. In Proceedings of the 14th Meeting of the International Committee on Global Navigation Satellite Systems, Bengaluru, India, 8–13 December 2019.
32. Estey, L.H.; Meertens, C. TEQC: The multi-purpose toolkit for GPS/GLONASS data. *GPS Solut.* **1999**, *3*, 42–49. [CrossRef]
33. Zhou, S. Studies on Precise Orbit Determination Theory and Application for Satellite Navigation System with Regional Tracking Network. Master's Thesis, University of Chinese Academy of Sciences, Beijing, China, 2011.
34. Dach, R.; Schaer, S.; Arnold, D.; Kalarus, M.S.; Prange, L.; Stebler, P.; Villiger, A.; Jäggi, A. *CODE Final Product Series for the IGS*; University of Bern: Bern, Germany, 2016; pp. 1–2.
35. Reischung, P.; Schmid, R. IGS14/igs14.atx: A new framework for the IGS products. In Proceedings of the American Geophysical Union Fall Meeting, San Francisco, CA, USA, 12–16 December 2016.
36. Flechtner, F.M.; Dahle, C.; Neumayer, K.H.; König, R.; Förste, C. The release 04 CHAMP and GRACE EIGEN gravity field models. In *Geological Storage of CO<sub>2</sub>—Long Term Security Aspects*; Springer International Publishing: Basel, Switzerland, 2010; pp. 41–58.
37. Standish, J.P.L. Planetary and lunar ephemerides, DE405/LE405. In *JPL Interoffice Memorandum 312.F-98-048*; Jet Propulsion Laboratory: Pasadena, CA, USA, 1998.
38. Petit, G.; Luzum, B. *Technical Report: IERS Conventions*; Verlag des Bundesamts für Kartographie und Geodäsie: Frankfurt am Main, Germany, 2010.
39. Lyard, F.; Lefevre, F.; Letellier, T.; Francis, O. Modelling the global ocean tides: Modern insights from FES2004. *Ocean Dyn.* **2006**, *56*, 394–415. [CrossRef]
40. Rosengren, A.J.; Scheeres, D.J. Long-term dynamics of high area-to-mass ratio objects in high-Earth orbit. *Adv. Space Res.* **2013**, *52*, 1545–1560. [CrossRef]
41. Picone, J.M.; Hedin, A.E.; Drob, D.P.; Aikin, A.C. NRLMSISE-00 empirical model of the atmosphere: Statistical comparisons and scientific issues. *J. Geophys. Res. Space Phys.* **2002**, *107*. [CrossRef]

42. Neumayer, K.; Michalak, G.; König, R. On calibrating the CHAMP on-board accelerometer and attitude quaternion processing. In *Earth Observation with CHAMP: Result from Three Years in Orbit*; Reigber, C., Lühr, H., Schwintzer, P., Wickert, J., Eds.; Springer: Berlin, Germany, 2005; pp. 71–76.
43. Chen, L.; Jiao, W.; Huang, X.; Geng, C.; Ai, L.; Lu, L.; Hu, Z. Study on signal-in-space errors calculation method and statistical characterization of beidou navigation satellite system. In *China Satellite Navigation Conference (CSNC) 2013 Proceedings*; Lecture Notes in Electrical Engineering; Springer: Berlin, Germany, 2013; Volume 243, pp. 423–434.
44. Xia, Y.; Liu, X.; Guo, J.; Yang, Z.; Qi, L.; Ji, B.; Chang, X. On GPS data quality of GRACE-FO and GRACE satellites: Effects of phase center variation and satellite attitude on precise orbit determination. *Acta Geod. Geophys.* **2021**, *56*, 93–111. [[CrossRef](#)]